Coordination Chemistry Reviews 319 (2016) 180–195

Contents lists available at ScienceDirect

Coordination Chemistry Reviews

journal homepage: www.elsevier.com/locate/ccr

Review

Stimuli–responsive metallopolymers

Kenneth Yin Zhang[a], Shujuan Liu[a], Qiang Zhao[a,*], Wei Huang[a,b,*]

[a] Key Laboratory for Organic Electronics and Information Displays and Institute of Advanced Materials (IAM), Jiangsu National Synergetic Innovation Center for Advanced Materials (SICAM), Nanjing University of Posts and Telecommunications (NUPT), Nanjing 210023, PR China
[b] Key Laboratory of Flexible Electronics (KLOFE) and Institute of Advanced Materials (IAM), Jiangsu National Synergetic Innovation Center for Advanced Materials (SICAM), Nanjing Tech University (NanjingTech), Nanjing 211816, PR China

Contents

ARTICLE INFO

Article history:
Received 26 January 2016
Accepted 29 March 2016
Available online 23 April 2016

Keywords:
Imaging reagent
Metallopolymer
Sensor
Stimuli–responsive materials

ABSTRACT

Stimuli–responsive metallopolymers have been drawing great research interest in the design and development of novel sensory materials. Smart metallopolymers combining advantages of both metal complexes and polymers exhibit good solubility and processibility, and show changes in conformation, conductivity, color, and luminescence in response to external stimuli. This review article summarizes the recent development of metallopolymers that are responsive to environmental physical parameters such as temperature, electricity, and light and chemical analytes such as pH values, ions and gas molecules. The applications of these stimuli–responsive metallopolymers as biological sensors and imaging reagents in biological environments have also been discussed.

Abbreviations: bpy, 2,2′-bipyridine; CT, charge-transfer; Cys, cysteine; DFT, density functional theory; dpbp, 4,4′-bis(diphenylphosphoryl)biphenyl; DTE, 1,2-bis(5-carboxyl-2-methyl-3-thienyl)perfluorocyclopentene; ECL, electrogenerated chemiluminescence; FRET, fluorescence resonance energy transfer; Hcy, homocysteine; hfa, hexafluoro acetylacetonato; ICP-MS, inductively coupled-plasma mass spectrometry; IL, intraligand; LCST, lower critical solution temperature; LMCT, ligand-to-metal charge-transfer; MLCT, metal-to-ligand charge-transfer; NIR, near infrared; PB, Prussian blue; PET, photoinduced electron transfer; PFO, poly(9,9-dioctylfluorene); PLIM, photoluminescence lifetime imaging microscopy; PVP, poly(*N*-vinylpyrrolidone); TBDPS, *tert*-butyldiphenylsilyl; TPrA, tri-*n*-propylamine; TTA, 2-thenoyltrifluoroacetone; UCST, upper critical solution temperature; UV, ultraviolet; WORM, write-once read-many times.

* Corresponding authors at: Key Laboratory for Organic Electronics and Information Displays and Institute of Advanced Materials (IAM), Jiangsu National Synergetic Innovation Center for Advanced Materials (SICAM), Nanjing University of Posts and Telecommunications (NUPT), Nanjing, 210023, PR China.
E-mail addresses: iamqzhao@njupt.edu.cn (Q. Zhao), wei-huang@njtech.edu.cn (W. Huang).

http://dx.doi.org/10.1016/j.ccr.2016.03.016
0010-8545/

1. Introduction

Smart functional materials that are capable of responding to external stimuli have recently become hot topics in the development of optical and electrical devices, sensors, and biomaterials [1–10]. The physical and chemical characteristics of these smart materials can be sensitively and reversibly altered by external stimuli and analytes. Novel stimuli–responsive materials include those of small molecules, polymers, and hybrids [1–10]. Polymers containing metal elements, especially those appearing in the repeating units, have received particular attention since they not only simply combine advantageous properties of both metal complexes and polymers, but also show new attractive properties that do not appear in metal complexes or organic polymers [11–20]. Metals are coordinated either in the polymer backbone or in the side chains and the shape of metallopolymers can be linear or highly branched. Generally, organic polymers impart solubility and processibility to the materials, while incorporation of metal atoms offers various functionalities including electrochromism, luminescence, redox, catalysis, *etc.* Owing to their interesting properties, metallopolymers have been widely applied in polymer light-emitting diodes, memory devices, solar cells, and drug carriers [11–29]. Recently, stimuli–responsive metallopolymers have been drawing much attention in the design and development of novel sensory materials. They undergo relatively large changes in response to small external stimuli or changes in their surrounding environment. Importantly, cooperation of coordination metals and polymer chains generates new responsive properties. For example, the luminescence properties of embedded metal complexes depend on the conformation of the polymer chain, and the content of the metals affects the gelation process of the polymer. Additionally, the multiple coordination bonds of metal centers allow crosslinking of polymer chains. Hence, triggering the break and restore of the coordination bonds offers new sensing strategies. With a judicious design, metallopolymers can be engineered to respond to specific physical stimuli including temperature, electricity, light, and chemical analytes such as gas molecules, pH values, small molecular compounds, and biomacromolecules. Their response is usually reflected by changes in conformation, conductivity, color, and luminescence. Recently, luminescent coordination metal complexes have been applied for bioimaging in live cells and small animals owing to their high luminescence quantum yields, large Stokes' shifts, high photostability, and good cell-membrane permeation [30–40]. Luminescent metallopolymers have also been applied for this purpose and exhibit several attractive advantages over other types of dyes. For example, it is very easy to improve the water solubility and biocompatibility via side chain modification. The long-lived luminescence of coordination metal complexes is easy differentiated from autofluorescence in biological samples via time-resolved luminescence imaging techniques.

In this Review article, we focus on responsive metallopolymers that contain repeating coordination metal complexes. The responsive behavior of these metal-containing polymeric materials toward physical stimuli such as temperature, electricity, light and chemical analytes such as pH values, ions, gas molecules has been discussed with emphasis on their design strategies and sensing mechanisms. The cooperation of polymer backbones and coordination metal complexes in converting the external stimuli into reporting signals has been highlighted. Applications of these responsive materials as biological sensors and bioimaging reagents in biological environments are also summarized.

2. Metallopolymers that are responsive to physical stimuli

2.1. Temperature responsive metallopolymers

Temperature is one of the most widely-used stimuli because it is easy to control and conveniently applied to different types of materials including biological samples. It is a common phenomenon that many organic polymers exhibit a LCST and/or UCST, at which the miscible polymer solution is sharply converted into non-soluble system upon increasing and decreasing temperature, respectively. Metallopolymers involving coordination metal complexes in the backbone or side chains provide a new design strategy for temperature responsive materials. Since many transition-metal complexes [30–38] and lanthanide chelates [39,40] display luminescence that is highly dependent on their microenvironment, temperature-induced conformational conversions of polymers can lead to changes in photophysical properties of these complexes. For example, Nitschke and co-workers have reported a temperature-responsive material involving a copper(I)-containing conjugated metallopolymer (**MP1**) with each copper(I) center coordinated with the diimine moiety in the polymer backbone and two individual phosphine ligands as $[Cu(N\hat{N})P_2]^+$ [41]. Unlike most gel-forming polymers, which undergo gelation upon cooling, **MP1** underwent sol-to-gel transition as the temperature was raised to 140 °C. The binuclear analogue did not show similar gelation behavior at such or higher temperature. The authors have proposed a mechanism for this counterintuitive high-temperature-induced sol-to-gel transition, which involves the reversible formation of $[Cu(N\hat{N})_2]^+$ cross-linkers as $2[Cu(N\hat{N})P_2] \rightleftharpoons [Cu(N\hat{N})_2] + [CuP_n] + (4-n)$ P. As the temperature was raised, the equilibrium favored the right-hand side and the resulting $[Cu(N\hat{N})_2]$ cross-linked polymer chains which led to sol-to-gel transition (Fig. 1). Accompanied with

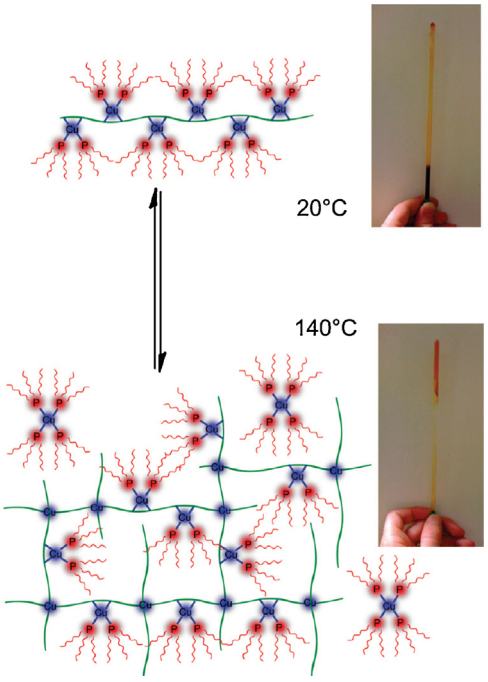

Fig. 1. Schematic representation of the gelation mechanism of **MP1** (left); photographs of inverted NMR tubes showing **MP1** in solution (top right) and following the sol-to-gel transition (bottom right).

Reprinted with permission from Ref. [41]. Copyright 2011, American Chemical Society.

the temperature-induced conformational change, the MLCT-based absorption band of **MP1** at 455 nm underwent hypochromic shift with a blue shift to 400 nm. The hypochromic shift has been attributed to the conversion of the colored $[Cu(N\hat{N})P_2]$ to the colorless $[CuP_n]$, and the blue shift was consistent with the fact that $[Cu(N\hat{N})_2]$ absorbs at a higher energy than $[Cu(N\hat{N})P_2]$. Additionally, **MP1** exhibited photoluminescence at 525 nm and 673 nm originated from IL and MLCT excited states, respectively. As the temperature increased, the MLCT-based emission band was preferentially quenched, which led to sharp changes in luminescence color from orange to green. In this example, the coordination copper(I) complex stabilized the polymeric imine ligand, and they cooperatively contributed to the interesting temperature induced conformational conversion and hence the absorption and luminescence response. A structurally-related metallopolymer **MP2** exhibited similar sol-to-gel transition upon increasing the temperature, and the emission maximum of **MP2** changed from 780 to 580 nm due to the loss of the copper phosphine complex from the polymer at a high temperature [42]. When **MP2** was fabricated into a light-emitting electrochemical cell, the electroluminescence color was dependent on the applied voltage, since a high voltage also triggered the release of the copper phosphine complex.

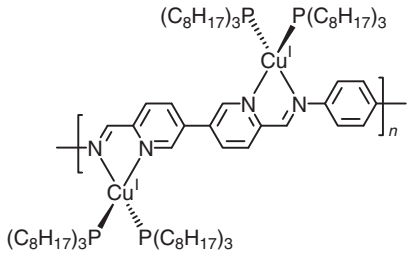

MP1

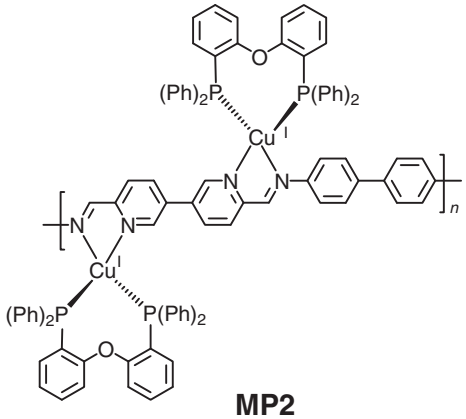

MP2

In another example, Hasegawa and co-workers have designed a lanthanide coordination polymer $[Tb(hfa)_3(dpbp)]_n$ (**MP3**) which exhibited temperature-dependent luminescence [43]. Since the energy level of the emissive state of Tb^{3+} (20,500 cm^{-1}) is close to that of the triplet state of the hfa ligand (22,000 cm^{-1}), back energy transfer occurred from sensitized Tb^{3+} to the triplet state of hfa. Increasing temperature facilitated this back energy transfer, and therefore dramatically quenched the luminescence of **MP3**. Incorporation of europium ion into the polymer system yielded the ratiometric temperature sensor $[Tb_{0.99}Eu_{0.01}(hfa)_3(dpbp)]_n$ [43]. The luminescence of Tb^{3+} ($^5D_4 - {}^7F_5$) and Eu^{3+} ($^5D_0 - {}^7F_2$) occurred at 543 nm and 613 nm, respectively. Upon increasing temperature, favored terbium-to-europium energy transfer led to quenching of the green terbium(III) luminescence and enhancement of the red europium(III) luminescence. As a consequence, solid-state **MP3** displayed brilliant green, yellow, orange, and red photoluminescence at 250, 300, 350, and 400 K, respectively, demonstrating color tuning of the coordination polymers in response to temperature changes.

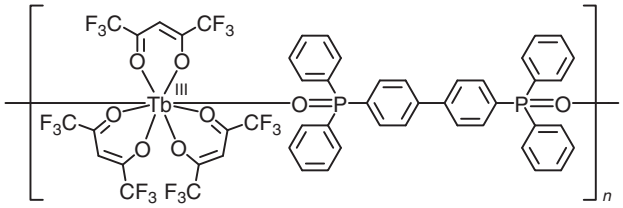

MP3

A ruthenium(II)-containing polyalkylacrylamide-based microgel (**MP4**) underwent the swell-collapse transition when the temperature increased across the volume phase transition temperature due to a change in the polymer-solvent affinity [44]. Accompanied with the transition, the diameter of the microgel particles considerably decreased, which shortened the average distance between adjacent ruthenium(II) complex cores. This conformational change did not specifically affect the photoluminescence of **MP4**. However, with TPrA as a coreactant, the ECL at 1.2 V vs. Ag/AgCl, which originated from the MLCT emissive state of $[Ru(bpy)_3]^{2+}$ generated via annihilation between $[Ru(bpy)_3]^{+}$ and $[Ru(bpy)_3]^{3+}$, was significantly enhanced by up to 100 folds. A higher molar percentage of ruthenium(II) complex moiety in the microgels gave a larger ECL enhancement factor. Such ECL amplification has been ascribed to the favored electron-transfer processes in the collapsed microgels. In this example, the successful demonstration of the extremely-rare turn-on luminescence with increasing temperature is attributed to rational combination of the photochemical and photophysical behaviors of transition-metal complexes and conformational properties of polymers.

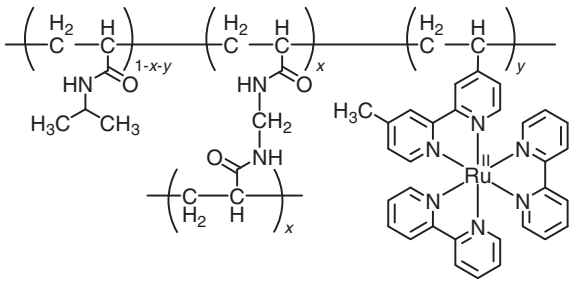

MP4

2.2. Electric responsive metallopolymers

2.2.1. Electrochromic metallopolymers

Electrochromic materials that exhibit reversible color change under electric stimuli have been widely used in electronic display devices [45–47]. Electrochromism usually occurs in π-conjugated polymers due to the reversible transition between two redox states [46–50]. Selective control of the redox state of each electrochrome under certain potentials allows the generation of individual electrochrome colors. The rich redox properties of coordination metal

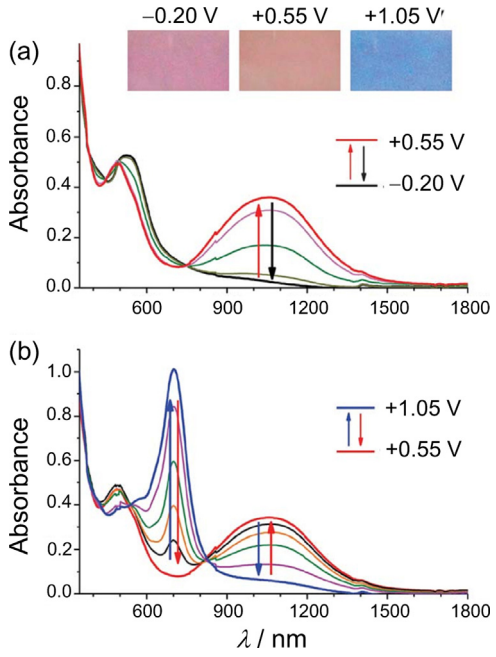

Fig. 2. Absorption spectral and color changes of **MP6**/ITO film upon (a) single oxidation and (b) double oxidation during spectroelectrochemical measurements. The applied potentials are referenced vs. Ag/AgCl.

Reprinted with permission from Ref. [52]. Copyright 2014, Royal Society of Chemistry.

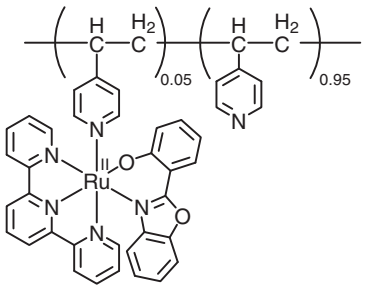

MP5

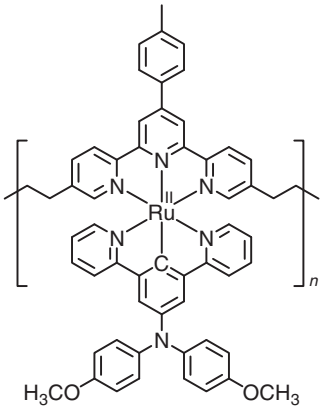

MP6

complexes allow metallopolymers to serve as multicolored electrochromic materials because of their multiple redox states. For example, a ruthenium(II)-containing poly(4-vinylpyridine)-based metallopolymer has been designed as a three-color electrochromic material (**MP5**) [51]. The reversible oxidation of the ruthenium(II) centers occurred at about 0.4 V vs. Ag/AgCl. Under a voltage of 0.5 V, the metallopolymer in thin film state exhibited a sharp color change from wine red to light green because the ruthenium(III/II)-based oxidation led to a hypochromic shift of the MLCT-based absorption band at 480 nm and a newly formed broad band centered at 760 nm, which has been assigned to the LMCT transition involving the negatively-charged phenolate ligand. A red orange color was also observed for mixed redox composition. Further oxidation at 1.5 V did not cause visible color change but resulted in disappearance of the LMCT absorption band at 760 nm because of irreversibly cleaving of the Ru–O bond. Although the second oxidation leading to absorption change in the NIR region cannot be discerned by naked eyes, this metallopolymer is useful for many practical applications. Another polymeric ruthenium(II) complex (**MP6**) displayed two oxidation processes accompanied with NIR electrochromism upon electric stimuli [52]. The first oxidation couple at 0.32 V vs. Ag/AgCl has been assigned to the oxidation of the triarylamine group to the ammonium radical cation, which gave rise to the formation of an intense absorption band at 1070 nm originating from a Ru → N^+ CT transition (Fig. 2a). In the process of ruthenium(III/II) oxidation, this band disappeared and a sharp absorption peak at 700 nm appeared owing to the N^+-localized $\pi \rightarrow \pi^*$ transition (Fig. 2b). As a result, the metallopolymer was purple, brown, and sky blue in color when a voltage of −0.20, +0.55, and +1.05 V, respectively, was applied. By using these potentials as inputs and the reading of the absorbance at 700 nm and 1070 nm as outputs, **MP6** has been used as a molecular platform for volatile memory devices. With an additional intermediate state between the two oxidized states under +0.80 V, the authors have demonstrated a multi-valued logic system.

Another general strategy to design multicolor electrochromism materials is incorporation of two or more different coordination metal centers into the same metallopolymers. Higuchi and coworkers have demonstrated the three-color electrochromism of a series of iron(II)/ruthenium(II)-based bimetallopolymers (**MP7**) with the molar ratio of Fe/Ru varying from 0 to 1 [53]. The MLCT absorption for iron(II) and ruthenium(II) centers occurred at 585 nm and 508 nm, respectively. These two absorption bands started to decrease in absorbance when the oxidation of iron(II) and ruthenium(II) occurred under a voltage of 0.7 V and 0.8 V, respectively. They are completely disappeared at 0.9 V and 1.1 V, respectively. These metallopolymer films exhibited high optical contrast and very short response time.

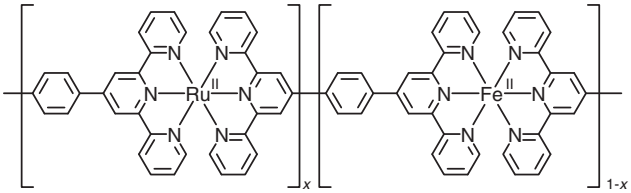

MP7

In the above examples, the multicolored electrochromism results from the multiple redox states of coordination complexes in the metallopolymers. The following example reports a new strategy that enables color mixing using a single working electrode. The ruthenium(II)-containing metallopolymer nanosheet (**MP8**) was sandwiched by two layers of PB-containing nanosheet [54]. PB is a well-known electrochromic materials with the formula of $KFe^{III}[Fe^{II}(CN)_6]$. Its oxidized form is $Fe^{III}[Fe^{III}(CN)_6]$ (PY)

which is yellow in color. When a voltage was applied to the trilayer film, the PB layer (PB1) directly contacted to the electrode was firstly oxidized to PY1. As the applied voltage increased, $[Ru(bpy)_3]^{2+}$ was oxidized to $[Ru(bpy)_3]^{3+}$, which catalyzed the oxidation of the other PB layer (PB2) to PY2. During the reverse scan, PY1 and $[Ru(bpy)_3]^{3+}$ was reduced, while the PY2 layer remained in the oxidized state. This work demonstrated the coexistence of an electrochromic material in different redox states at a single working electrode, which allowed multiple colors to be displayed.

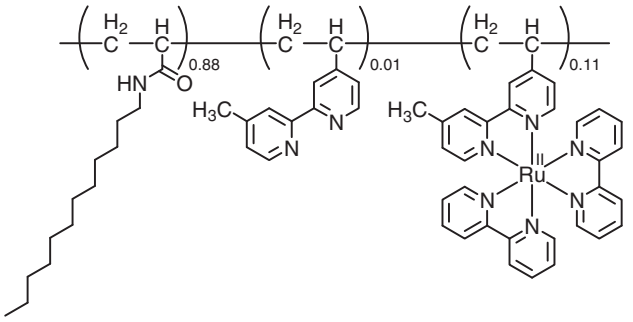

MP8

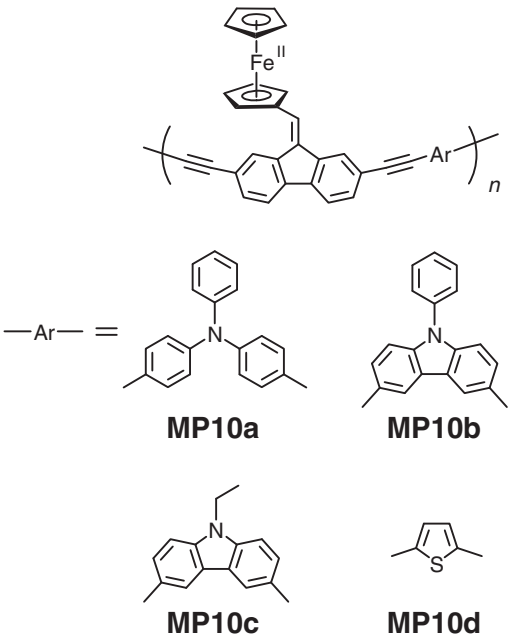

2.2.2. Metallopolymers for memory applications

Materials that show reversible redox response to electric stimuli are also promising candidates for memory applications because they provide the bistability that allows data to be stored as "0" and "1". Ferrocene has been widely employed in the design of memory materials as it undergoes a reversible one-electron oxidation to ferrocenium at a low potential. For example, a memory device was fabricated by spin-coating a ferrocene-containing conjugated polymer (**MP9**) in chlorobenzene onto the ITO patterned glass followed by vacuum deposition of a lithium fluoride layer and covered with aluminum as the top electrode [55]. **MP9** switched from a low-conducting state to a high-conducting state at a bias of −1.9 V because of the oxidation of ferrocene moieties. The reverse process was triggered at a bias of +1.4 V. A high on/off ratio up to 10^3 was obtained. The memory device performance of ferrocene-containing poly(fluorenylethynylene)s **MP10a–MP10d** depended on the chemical structures of the aromatic components in the polymer backbone [56]. **MP10a–MP10c** containing mainchain triphenylamine, phenylcarbazole, and ethylcarbazole, respectively, exhibited typical flash memory properties due to their electrical bistability. In contrast, **MP10d** containing thiophene displayed WORM memory properties. Theoretical DFT calculation and electrochemical investigations indicated that the different memory behavior of **MP10d** probably resulted from polymer aggregation induced by electrochemical coupling of the thiophene units. In addition to physical electric stimuli, ferrocene-containing metallopolymers exhibit redox response to different oxidants and reductants [57–59]. Compared to redox chemical reactions, electric responsive materials provide fast and reversible switching between oxidized and reduced states.

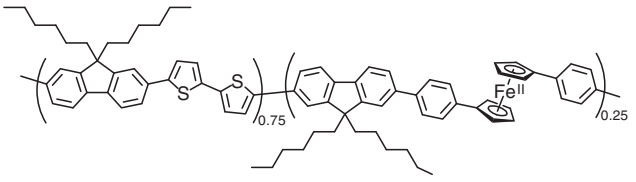

MP9

Conjugated metallopolymers that can be excited to a CT (between the polymer backbone and the metal complexes) state under specific voltages can be used as active materials in memory devices. For example, two conjugated polymers **MP11a** and **MP11b** containing iridium(III) complexes in the side chains was, respectively, spin-coated as the active layer sandwiched between an aluminum electrode and an indium tin oxide electrode [60]. Both metallopolymers reached a backbone-to-iridium(III) CT state under an electric-stimulus at −1.2 V and −1.4 V, respectively, which switched the metallopolymers from a low-conducting state to a high-conducting state. A reverse bias was required to turn off the CT state. An on/off current ratio of about 10^3 was obtained and the on and off states are stable up to 10^7 read cycles at a read voltage of −1.0 V. In another work of the same group, **MP12–MP14** involving an iridium(III) complex in the main chain of polyfluorene exhibited an on/off ratio up to 10^5 and the stability of both states was increased by 10 folds [61]. Similar metallopolymer containing side-chain (**MP15** and **MP16**) [62] and on-chain (**MP17**) [63] platinum(II) complexes have also been used as active materials in resistive random-access memory devices. Results showed that the devices using polycarbazole platinum(II) metallopolymer as the active material exhibited a lower threshold voltage and a higher on/off current ratio compared to that using a polyfluorene based metallopolymer.

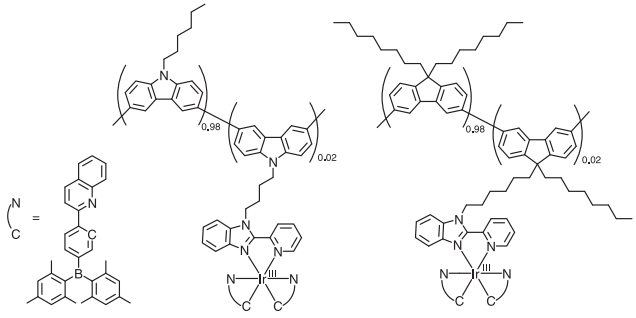

MP11a **MP10b**

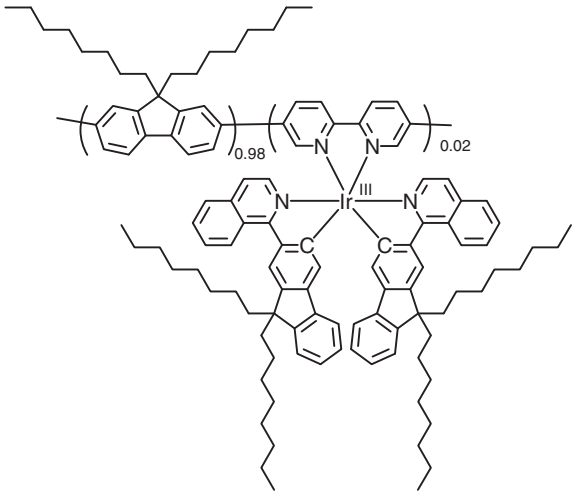

MP12

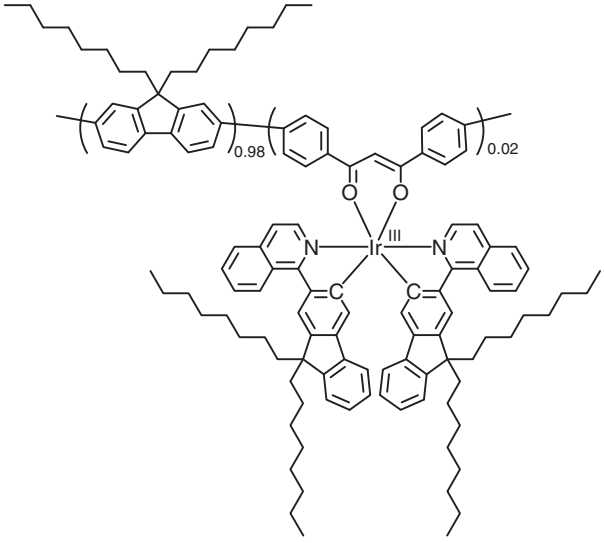

MP13

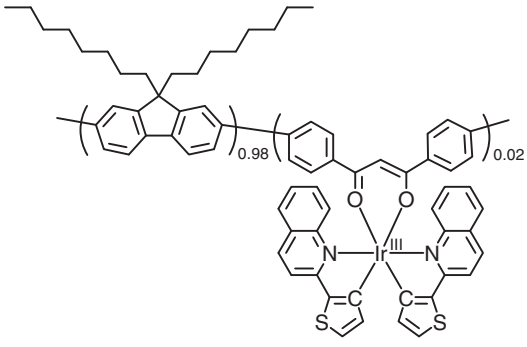

MP14

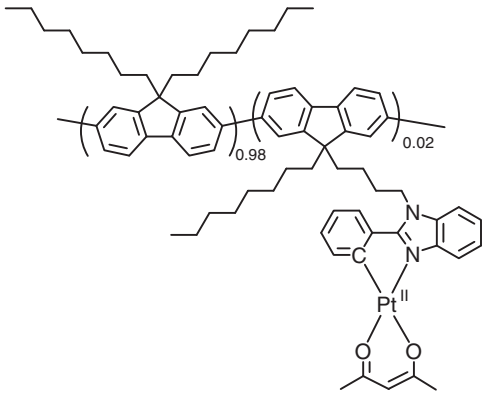

MP15

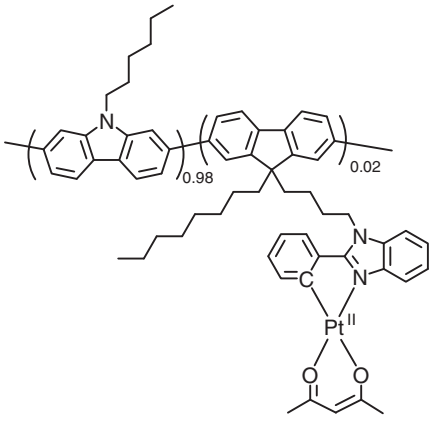

MP16

Non-conjugated polymers containing pendant carbazole moieties have been reported to display conformation-induced electrical bistability [64]. Since carbazole is also a well-known electron-donor, incorporation of coordination metal complexes pendants as the electron-acceptor into the polymer allows CT from the carbazole to the coordination complexes, which enables a ternary memory device. A ternary electronic memory device has been designed by using an iridium(III)-containing carbazole-based non-conjugated polymer (**MP18**) as an active material [65]. Oxidation of the carbazole pendant at a bias of −0.55 V gave rise to a conformational change and switched the metallopolymer from a low-conducting state to a high-conducting state (Fig. 3). A carbazole-to-iridium CT state was reached when the bias was increased to −1.15 V, which further promoted the metallopolymer to a higher-conducting state. A reverse bias at +2.5 V directly switched the higher-conducting state to the low-conducting state. **MP18** at the low-, high-, and higher-conducting states showed a conductivity ratio of $1{:}10^{-1.5}{:}10^{-4.5}$, which acted as “0”, “1”, and “2” states for digital memory. As a result, compared to a binary memory device, a ternary one significantly enlarges the memory capacity from 2^n to 3^n.

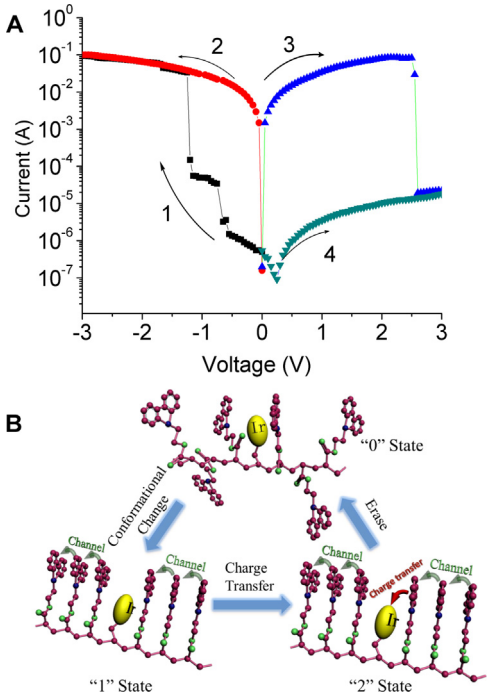

Fig. 3. (A) Typical *I–V* characteristics of a memory device containing **MP18**. (B) The proposed memory mechanism for the ternary memory behavior of **MP18**.
Reprinted with permission from Ref. [65]. Copyright 2012, Wiley-VCH.

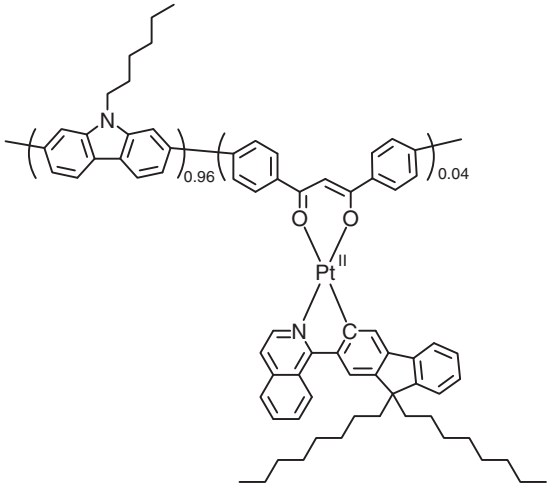

MP17

2.3. Light responsive metallopolymers

Materials able to respond to light irradiation usually undergo photochemical reactions, such as photo-induced isomerization and elimination, upon exposure to light of a specific wavelength [66–68]. Azobenzene [69,70] and diarylethene [70–72] derivatives are two major family of light responsive materials that readily undergo reversible photo-induced isomerization. Bellemin-Laponnaz, Mauro, and co-workers prepared a metallopolymers **MP19** based on zinc(II) terpyridine coordination nodes via heating $Zn(BF_4)_2$ in the presence of ditopic tpy ligands containing a photoisomerizable azobenzene unit and a solubilizing phenyleneethynylene moiety, respectively, with a molar ratio of these two ligands of 2:1 [73]. In DMF solution, the trans-to-cis isomerization

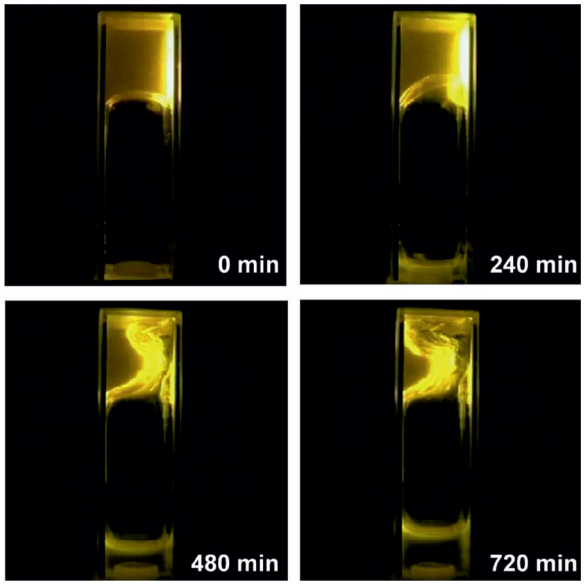

Fig. 4. Contraction of the **MP19** gel upon continuous UV photoirradiation (λ_{ex} = 365 nm) showing the macroscopic photomechanical response.
Reprinted with permission from Ref. [73]. Copyright 2016, Wiley-VCH.

of **MP19** was achieved upon irradiation at 365 nm using a LED light source. The *trans* form was recovered upon irradiation under visible light at 455 nm. Additionally, **MP19** exhibited excellent gelation ability with a critical gelation concentration as low as 0.12 wt.% in DMF/EtOH (1: 20, v/v). The **MP19** gel showed self-healing property owing to the breakage and rebuilding of interchain interactions and ligand–Zn(II) bonds. Interestingly, irradiation of the gel (0.2 wt.% in DMF/EtOH 1:20, v/v) at 365 nm led to contraction of the gel by 85% of its initial volume (Fig. 4). Since ICP-MS analysis confirmed that the zinc concentration in the excreted solution was much lower (to be about 8%) than that in the original gel, the reason of the light-induced contraction of **MP19** gel has been attributed to a release of an excess of the solvent mixture during the *cis*-to-*trans* transition rather than a simple melting process. Yamashita and co-workers reported a two-dimensional dysprosium(III) coordination polymer **MP20** in which two Dy(III) ions were bridged by four carboxylato groups of the DTE ligands and each Dy(III) ion was coordinated with one oxygen atom of another DTE in a monodentate fashion [74]. Upon UV irradiation, the DTE ligand underwent ring-close isomerization, which not only caused the color change of **MP20** from colorless to deep blue, but also induced variation of the magnetic properties. In either open or closed forms, **MP20** exhibited slow magnetic relaxation without an external dc field. The magnetic properties of the Dy(III) complexes were affected by the photo-induced isomerization of the ligand, due to the change in the coordination sphere and the crystal field around the Dy(III) ions.

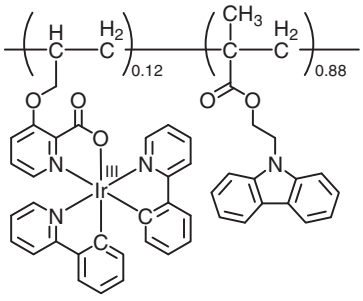

MP18

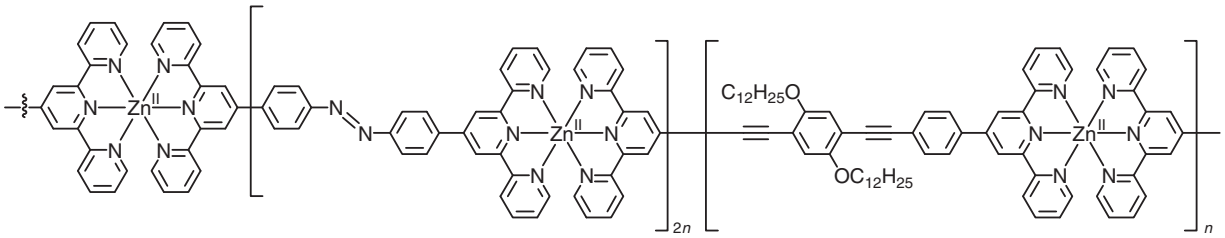

MP19

A bimetallopolymer **MP21** containing salen-zinc(II) and [Eu(bpy)(TTA)$_3$] monomers did not undergo any photochemical reaction, but its photoluminescence color was dependent on the excitation wavelength [75]. Upon photoexcitation at 430 nm, **MP21** exhibited orange luminescence at 556 nm, which has been assigned to the π–π^* transition of the zinc(II)-containing polymer backbone because the luminescence spectrum was almost identical to that of the Eu(TTA)$_3$-free analogue. When **MP21** was excited at 351 nm, characteristic red luminescence at 613 nm was observed, which has been assigned to $^5D_0 \rightarrow {}^7F_2$ transition of the europium(III) ions. Excitation at a wavelength between 365 nm and 400 nm resulted in emission of a mixed color. The variation in luminescence color is due to that high-energy excitation resulted in efficient sensitization of the europium(III) ions while low-energy excitation limited the energy transfer from the zinc(II)-containing polymer backbone to the europium(III) ions.

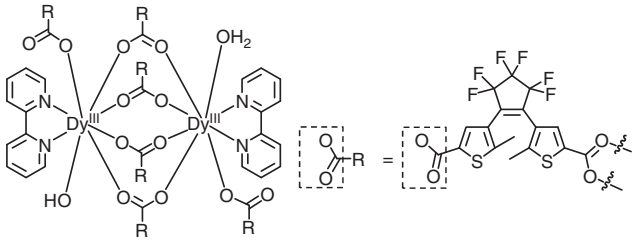

MP20

3. Metallopolymers that are responsive to chemical analytes

3.1. Metallopolymers that are responsive to pH values

Polymers that contain proton donating or accepting groups in their monomers commonly show pH-dependent solubility and gelation [76]. The most well-known example is that proteins mainly composed of acidic or basic amino-acids undergo precipitation at a low or high pH value. Redox-active polymers can respond to pH values in a different way. Lawrence and co-worker have reported a vinylferrocene- and vinylanthracene-based copolymer (**MP22**) that did not contain any protonating or deprotonating group [77]. Both monomers in this copolymer were redox active. Square-wave voltammograms showed that the reduction of vinylanthracene occurred at −0.69 V at pH 9, and this potential was linearly shifted to less negative by about 0.06 V when the pH value was decreased by every 1 unit from 9 to 4. The reason of this pH-sensitive redox behavior is that the two-electron reduction of vinylanthracene required involvement of two protons, and thus a lower pH value facilitated the reduction. Since the redox potential of vinylferrocene was independent of pH values, the signal of vinylferrocene can be used as an internal reference to improve the accurancy of the pH sensing. Additionally, the redox response toward pH values was stable over a wide temperature range.

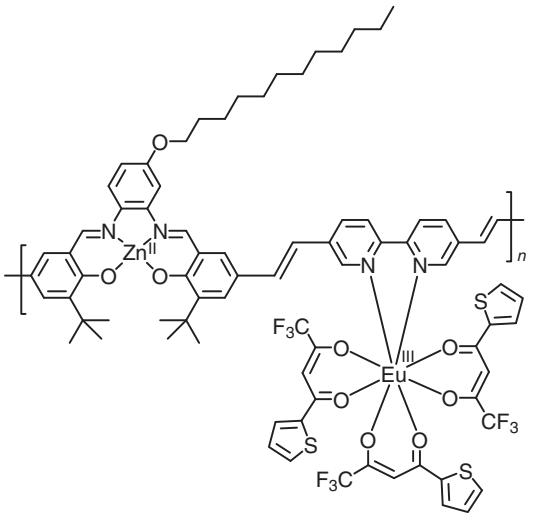

MP21

3.2. Metallopolymers that are responsive to gas molecules

The determination of oxygen concentrations in air, solutions and biological systems is important to biomedicine, industry, and environmental science. Phosphorescent transition-metal complexes have been widely used in the oxygen-sensing applications because of efficient quenching of their triplet states by molecular oxygen through triplet–triplet annihilation and a PET process [78]. As a result, these complexes display weaker emission with a shortened lifetime in the presence of molecular oxygen. The complexes are usually dissolved or immobilized in polymers for oxygen sensing [79]. Covalent attachment of transition-metal complexes to polymers can significantly improve the sensitivity to oxygen quenching compared to the case where the complexes are simply dissolved in the polymer films [80]. Additionally, coordination of transition-metal complexes with conjugated polymer elongates the triplet excited-state lifetimes due to the extension of the exciton length, which leads to increased sensitivity to trace oxygen. For example, a phosphorescent platinum(II)-containing conjugated poly(phenylene) **MP23** has been employed as an oxygen sensor [81]. This coordination metallopolymer exhibited phosphorescence at 585 nm with a lifetime as long as 14 μs. **MP23** showed a sensitivity improvement for dissolved oxygen quantification since its long excited state lifetime allows competitive diffusion of oxygen with their radiative rates. Another phosphorescent platinum(II)-containing conjugated polyfluorene **MP24** exhibited both fluorescence and phosphorescence from polyfluorene and the platinum(II) complex, respectively, and the phosphorescence lifetime was as long as 40 μs [82]. Under an

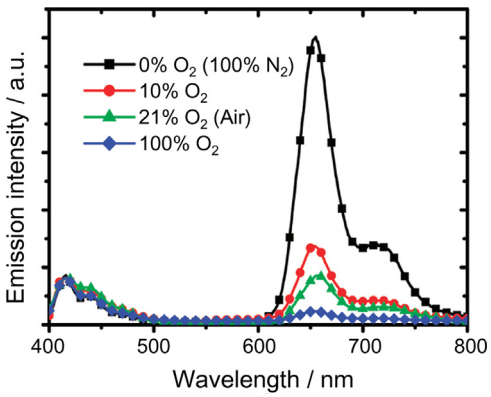

Fig. 5. Photoluminescence spectra of **MP24** in 1,2-dichloroethane at room temperature at various oxygen concentrations.
Reprinted with permission from Ref. [82]. Copyright 2012, American Chemical Society.

atmosphere of 100% oxygen, **MP24** displayed blue fluorescence with weak red phosphorescence due to the selective quenching of long-lived phosphorescence. With decreasing oxygen contents, the red phosphorescence was enhanced while the blue fluorescence was almost unchanged (Fig. 5), leading to a change of the total emission color from blue to red which could be recognized by the naked eye under UV excitation.

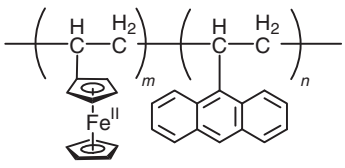

MP22

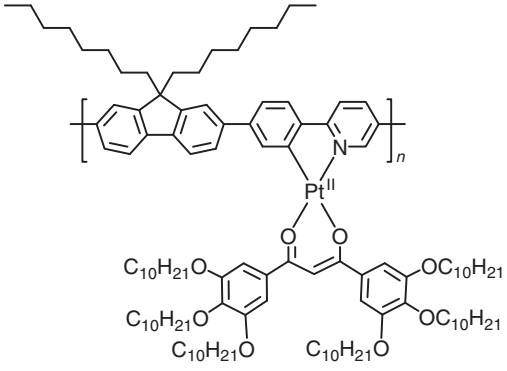

MP23

Nitric oxide (NO) is one of the most important cellular signaling molecules involved in many physiological and pathological processes [83–86]. Intracellular NO is difficult to be detected because of its low concentration and short half-life. Lippard and co-workers have designed a series of conjugated polymers (**P25**) whose emission was efficiently quenched upon coordination to copper(II) ions [87]. When copper(II) was reduced to copper(I) by NO, the emission of the polymers recovered, rendering these materials potential candidates for NO sensing by a turn-on emission mechanism. In another study of the same research group, hydrophilic groups were incorporated into the copper(II)-binding conjugated metallopolys, forming water soluble NO sensors (**P26**), which exhibited excellent selectivity and biocompatibility [88].

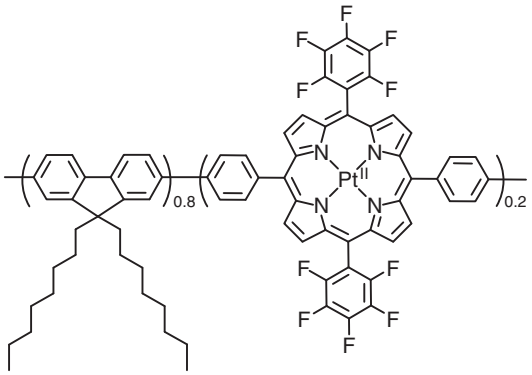

MP24

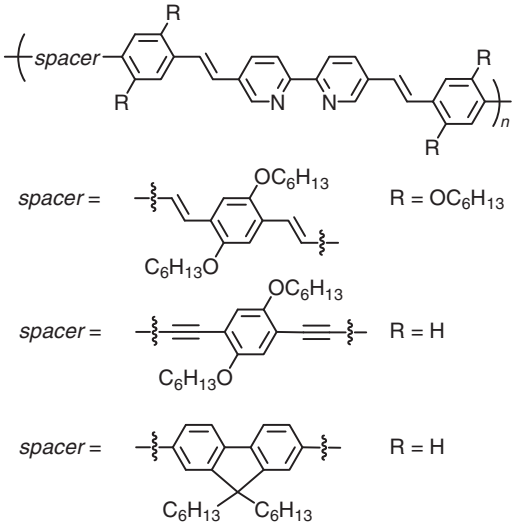

P25

Swager and co-workers have developed a cobalt(II)-containing conducting metallopolymer (**MP27**) which sensed NO in a different mechanism [89]. This metallopolymer was composed of coordinatively unsaturated cobalt(II) salphen (N,N′-propylenebis-(salicylidenimine)) complex and 3,4-(ethylenedioxy)thiophene as monomers. The well matched redox potentials of these two moieties made the metallopolymer highly conductive. Exposure of the material to NO gas resulted in an increase in electrical resistance due to coordination of NO to the cobalt(II) center. Although similar response was also observed toward NO_2, the bonding of NO is reversible whereas irreversible redox reaction occurred in the presence of NO_2 yielding Co(III) nitrite complex.

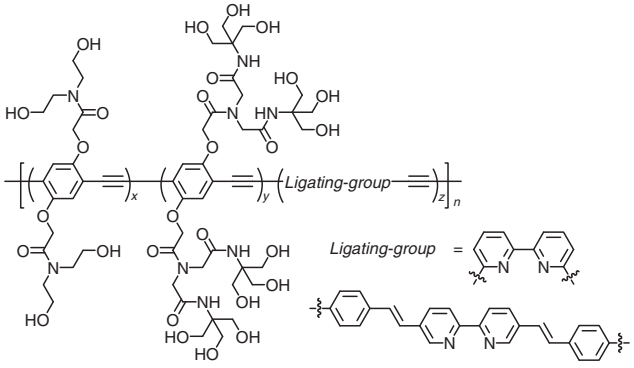

P26

Terao and co-workers have synthesized a molecular wire (**MP28**) with high linearity, rigidity, and intramolecular charge mobility through the coordination polymerization of ruthenium(II) porphyrin [90]. Interestingly, this metallopolymer-based wire underwent depolymerization under an atmosphere of carbon monoxide (CO), yielding a ruthenium(II) porphyrin carbon monoxide monomer because of the strong coordination ability of CO. UV irradiation triggered the release of CO and repolymerization of the molecular wire. Vancso and co-workers have reported a simple and fast electrografting method to chemically modify Au electrodes with a redox-active organometallic polymer **MP29** for the detection of ascorbic acid, which is one form of Vitamin C [91]. **MP29** effectively catalyzed the oxidation of ascorbic acid electrochemically under a voltage of 0.52 V (vs. Ag/AgCl), resulting in sensitive and reproducible amperometric response.

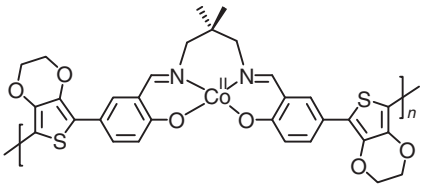

MP27

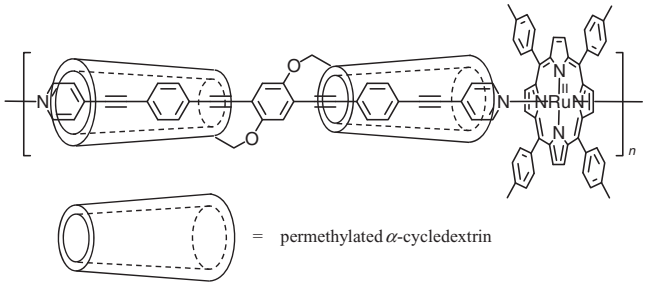

MP28

3.3. Metallopolymers that are responsive to ions

Many phosphorescent transition-metal complexes and luminescent lanthanide chelates have been designed as sensors for various anions and cations in solution and biological environment owing to their environment-dependent photophysical properties [30–40]. The advantages of these inorganic compounds include high emission quantum yields that enhance the detection sensitivity, large Stokes shifts that minimize self-quenching, and long emission lifetimes that facilitate time-resolved detection [30–40,92,93]. Incorporation of these inorganic complexes into conjugated polymers allows electronic communication between the complexes and polymer backbone, which provides new ion sensory mechanisms. For example, an iridium(III)-containing PFO-based conjugated polymer (**MP30**) has been synthesized as a Hg^{2+} sensor in solutions and films [94]. Upon photoexcitation, the emission of the PFO backbone and the iridium(III) complex occurred at 460 nm and 618 nm, respectively, and efficient Förster energy transfer from the PFO backbone to the iridium(III) complex occurred owing to the spectral overlap of the emission of the former and the absorption of the latter, resulting in predominance of the red emission color. Addition of Hg^{2+} led to decomposition of the iridium(III) complex units and cut off the energy transfer pathway, recovering the π–π* transition-based emission of the polymer backbone at 509 nm, which was greenish yellow in color. In another study, a hybrid complex composed of an anionic

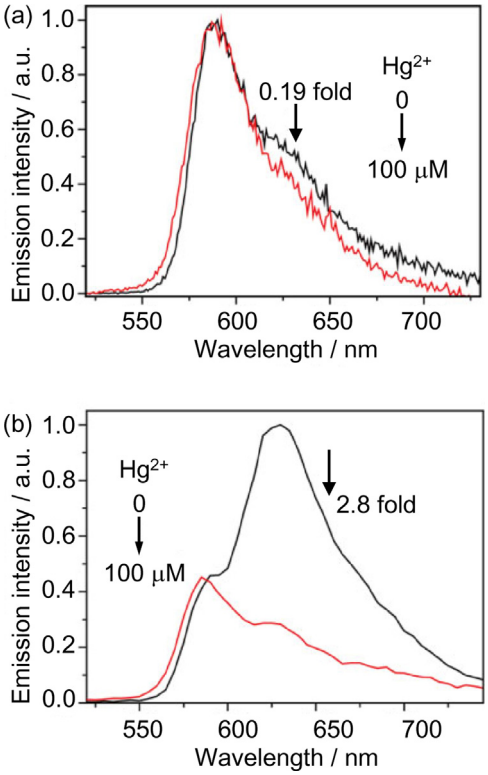

Fig. 6. Photoluminescence spectra of the hybrid complex of **M31** and **P31** in the presence of Rhodamine B upon addition of Hg^{2+} in (a) a steady state and (b) at delay time of 99 ns excited at 379 nm.

Reprinted with permission from Ref. [95]. Copyright 2013, Wiley-VCH.

conjugated polyelectrolyte (**P31**) and a cationic phosphorescent iridium(III) complex (**M31**) has been prepared via electrostatic attraction [95]. Efficient FRET from the anionic polymer to the cationic iridium(III) complex occurred in aqueous solution, but became inefficient in the presence of Hg^{2+}. Hence, addition of Hg^{2+} led to quenching of the luminescence of **M31**. The Hg^{2+} detection sensitivity of this hybrid complex is at least five-fold enhanced compared to that of the iridium(III) complex monomer. Additionally, the hybrid complex has been used to detect Hg^{2+} in the presence of Rhodamine B via time-resolved photoluminescence owing to the long-lived triplet emissive state of the iridium(III) complex **M31**. In contract to the steady-state spectra where the luminescence of **M31** was completely embedded into the intense fluorescence of Rhodamine B, the time-resolved luminescence spectra with a delay time of 99 ns recorded the luminescence response of **M31** to Hg^{2+} (Fig. 6). Chen and co-workers have developed a coordination polymer (**MP32**) composed of terbium(III) ion, adenine, and dipicolinic acid for Hg^{2+} sensing [96]. This coordination polymer emitted very weakly due to PET from adenine to dipicolinic acid, which prevents the sensitization of terbium(III) ion. In the presence of Hg^{2+}, the coordination polymer exhibited significant luminescence enhancement because of the suppression of the PET process by the coordination of Hg^{2+} with adenine.

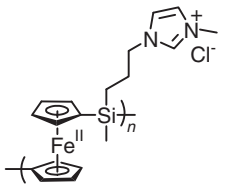

MP29

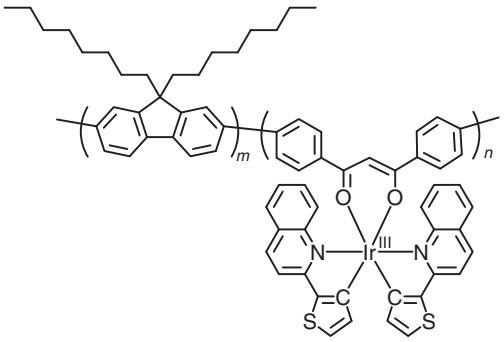

MP30

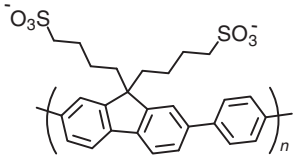

P31

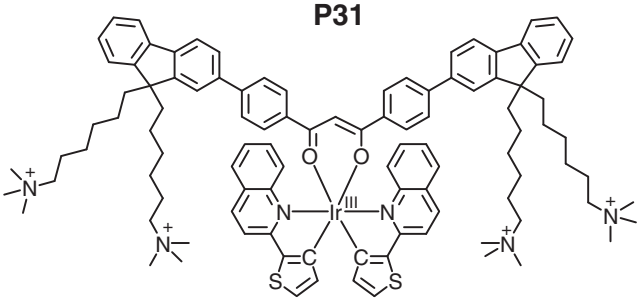

M31

Astruc and co-workers synthesized a biferrocene polymer **MP33** via click polymerization involving triazole formation from azides and alkynes [97]. **MP33** showed multifunctional properties as polyelectrolytes and electrochromes, electrode modifiers, and nanoparticle stabilizers for catalysis. Additionally, redox properties of **MP33** properties were sensitive to the palladium cation. The cylic voltammogram of **MP33** showed two reversible oxidation couples at 0.440 and 0.785 V vs. Fc^+/Fc. Addition of Pd^{2+} caused a splitting of the second oxidation wave, because of the coordination of Pd^{2+} to the nitrogen atoms of the triazole moiety, which modified the electron density of the Fc centers. Wong, Wang, and co-workers have designed a platinum(II)-containing polymer as a water soluble Ag^+ sensor (**MP34**) [98]. It exhibited a ^{1}IL absorption band at 390 nm which underwent significant red-shift to 480 nm in the presence of Ag^+ because of metal-cation-induced intersystem crossing from the singlet to triplet states.

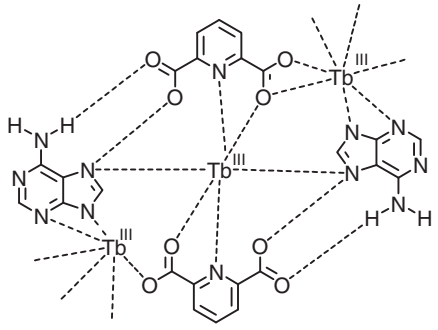

MP32

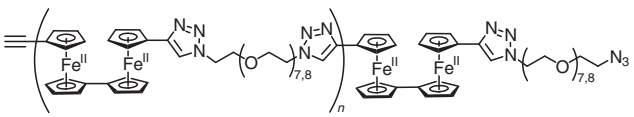

MP33

Poly[2,5-thiophenediyl-1,2-ethynediyl-1,4-phenylenediyl-1,2-ethynediyl] with a *N*,*N*,*N*′-trimethylethylenediamino as the recognizing units for cations on the thiophene ring (**P35**) showed small luminescence enhancement when exposed to most cations including Li^+, Na^+, K^+, Mg^{2+}, Ca^{2+}, H^+, Mn^{2+}, Fe^{2+}, Co^{2+}, Ni^{2+}, Zn^{2+}, Cd^{2+}, and Hg^{2+}, but significant luminescence quenching in the presence of Cu^{2+} [99,100]. Thus, a copper(II) coordination metallopolymer was prepared as a turn-on luminescence for other cations. Interestingly, this metallopolymer showed very high selectivity toward iron ions with no discrimination between ferrous and ferric ions. Compared to **P35**, the copper(II) coordination metallopolymer displayed sensitivity improved by over 2 orders of magnitude. A slight structural modification of the recognizing pendant with an additional methylene group yielded **P36** [100]. The luminescence at 490 nm was quenched by 88% in the presence of ferric ion. **P36** exhibited excellent selectivity toward ferric ion against other metal ions including Fe^{2+} and Cu^{2+}. The difference in response to ferric and ferrous ions has been attributed the harder nature and smaller size of Fe^{3+}, which facilitates the hard-hard interaction with the diamino-based receptor.

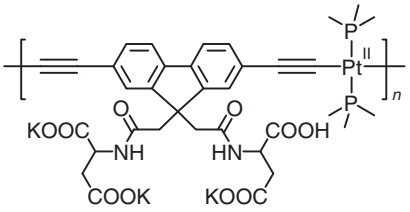

MP34

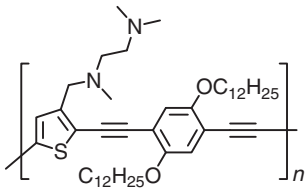

P35

4. Responsive metallopolymers as biological sensors and bioimaging reagents

The interesting sensory behaviors of responsive metallopolymers have prompted researchers to investigate their possible applications in biological systems. Xiao, Wang, Tian, and co-workers have developed platinum(II)-containing polymeric nanoprobes (**MP37**) for intracellular oxygen sensing [101]. The nanoprobes were prepared in a core-shell type with a platinum(II)-porphyrin-containing non-conjugated polymer as the hydrophobic core and 2,2′-*N*-isopropylacrylamide as the hydrophilic and biocompatible shells. The emission of the nanoprobes at 650 nm was

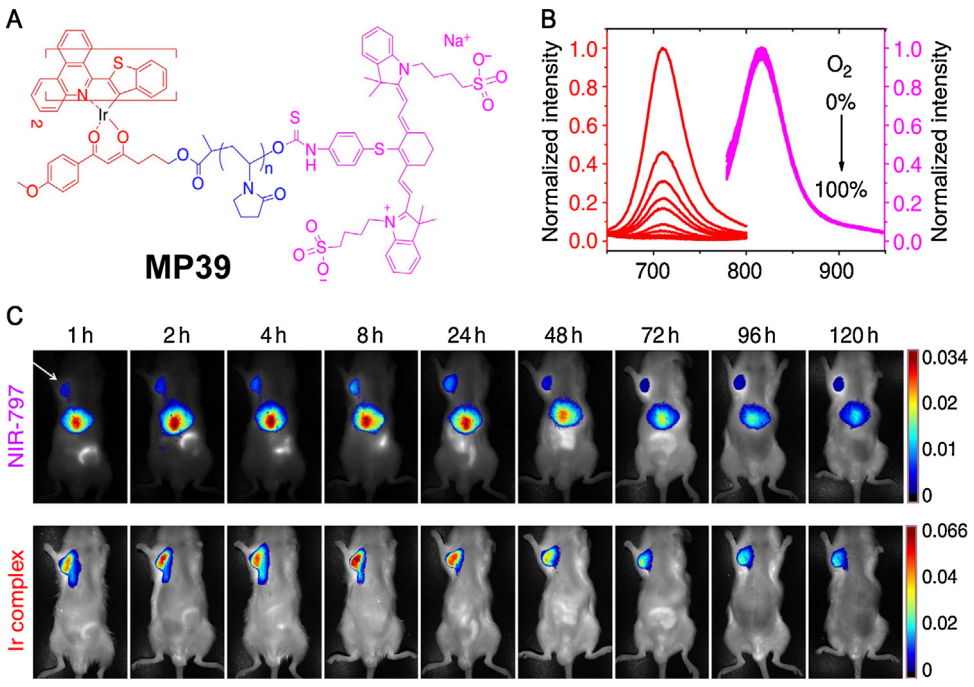

Fig. 7. (A) Chemical structure of Ir-PVP-N. (B) Emission response of **MP39** toward oxygen. (C) Whole-body optical images of ICR mice bearing subcutaneously implanted H22 tumors in the armpit after intravenous injection of **MP39** (40 mg kg^{-1}).
Reprinted with permission from Ref. [104]. Copyright 2015, Nature Publishing Group.

phosphorescence in nature and very sensitive toward oxygen quenching. The intracellular oxygen-sensing performance of the nanoprobes were investigated by using vero cells via confocal luminescence microscopy. Cells under a nitrogen atmosphere displayed intense phosphorescence, whereas the intensity decreased to below 40% when the cells were cultured in a 20% oxygen condition. Recently, the water-soluble platinum(II) porphyrin-fluorene metallopolymer **MP38** has been used for hypoxia bioimaging via photoluminescence lifetime imaging [102,103]. The average emission lifetime of live HepG2 cells treated with **MP38** was about 17 ns, which was elongated to 95 ns when the oxygen concentration was reduced to 2.5%. Additionally, the utilization of **MP38** for luminescence imaging of tumor hypoxia in nude mice was demonstrated. The mice were injected with **MP38** intratumorally and subcutaneously, respectively. Only the tumor area displayed intense luminescence from the platinum(II) porphyrin, indicative of the tumor hypoxia. More recently, Jiang and co-workers designed an iridium(III)–PVP NIR-797 (**MP39**) conjugate by modification linear PVP with an iridium(III) complex and the NIR-797 dye at the two terminal ends, respectively (Fig. 7A) [104]. The phosphorescence of the iridium(III) complex occurred at 710 nm while the NIR-797 dye emitted at 825 nm. The dual NIR emission gave rise to deeper tissue penetration compared to the emission in the visible region and facilitated the luminescence imaging in tissue and animal modes. As expected, only the phosphorescence was quenched by oxygen (Fig. 7B) and thus the signal from the NIR-797 moiety can be used as an internal standard to assess the probe concentration non-invasively *in vivo*. As shown in Fig. 7C, whole-body imaging of mice bearing subcutaneously implanted H22 tumours with signal from the NIR-797 moiety showed that there was a significant liver accumulation of the probe. In contrast, imaging with phosphorescence signal from the iridium(III) complex showed that the signal from the tumor was outstanding because of the rapid consumption of oxygen in the tumor.

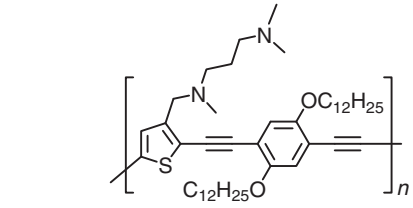

P36

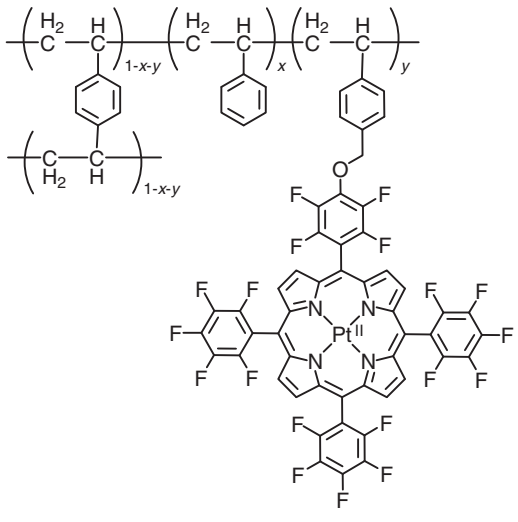

MP37

Fluoride is important in many health and environmental concerns. Reasonable water fluoridation and addition of fluoride to toothpaste have become a widespread practice due to the beneficial effects of fluoride on dental health and osteoporosis treatment

[105]. An iridium(III) complex containing a TBDPS moiety in each cyclometallating ligand exhibited sensitive and selective luminescence response toward fluoride, owing to the fluoride-induced release of the TBDPS units which triggered PET-based luminescence quenching of the excited iridium(III) complex [106]. Incorporation of this complex into polyflorene yielded a dual-luminescent conjugated metallopolymer **MP40**, which, upon photoexcitation, displayed blue (420 nm) and red (600 nm) luminescence from polyflorene and the iridium(III) complex, respectively. Addition of excess fluoride quenched the luminescence of the iridium(III) complex and the intensity ratio $I_{600\,nm}/I_{420\,nm}$ dropped from 2.03 to 0.66, resulting a luminescence color change from orange to blue. **MP40** was water soluble due to the presence of pendant quaternary ammonium moieties and has been used to image intracellular fluoride. HeLa cells were treated with **MP40** and the luminescence of polyflorene and the iridium(III) complex was analyzed via blue (410–480 nm) and red (560–650 nm) windows, respectively. Before loading of fluoride, intense luminescence was detected via both windows. Upon treatment of the cells with fluoride, the blue luminescence remained unchanged but the red luminescence became dim. The intensity ratio of these two windows, I_{red}/I_{blue}, decreased from 1.12 to 0.29, demonstrating ratiometric sensing of fluoride.

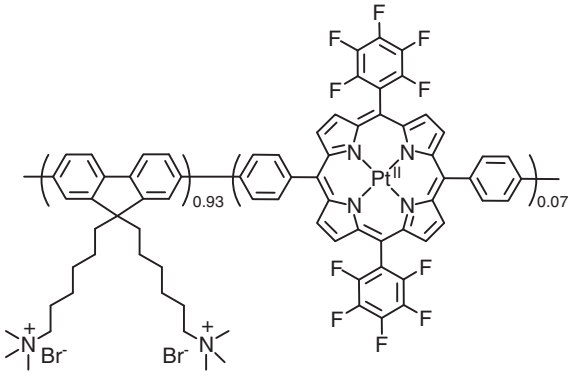

MP38

Hcy and Cys play important roles in metabolism of cells [107,108]. Organic fluorescent Cys sensors exhibted high sensitivity [109,110], but the short-lived fluorescence suffers from interference with autofluorescence. Transition-metal complexes bearing aldehyde groups have been used as Hcy/Cys sensors as the aldehyde groups can selectively react with Hcy/Cys over other amino acids, yielding cyclic thiazinane and thiazolidine derivatives, respectively [37,38]. However, their poor water solubility limits intracellular sensory applications. This problem can be addressed by incorporation of transition-metal complexes into water-soluble polymers. For example, two iridium(III) bisaldehyde complexes have been integrated into poly(*N*-isopropylacrylamide) [111,112]. The formed metallopolymers (**MP41** and **MP42**) displayed significant emission enhancement upon reacting with Hcy/Cys. Upon incubation with these metallopolymers, KB cells exhibited intense emission from cytoplasm. The emission originated from the thiazinane/thiazolidine products of the reaction between the iridium(III) bisaldehyde complexes and Hcy/Cys because the emission intensity was much lower when the cells were pretreated with *N*-ethylmaleimide which is a thio-reactive compound to consume Hcy/Cys. Additionally, PLIM which distinguishes the long-lived phosphorescence from short-lived fluorescence interference was, for the first time, employed for bioimaging of intracellular Cys [112].

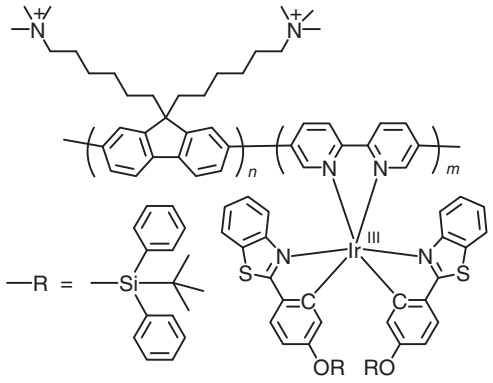

MP40

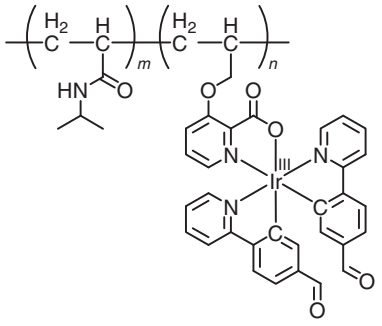

MP41

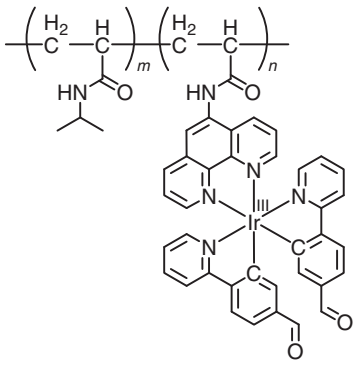

MP42

Heparin is a polyanionic biomacromolecule and its very high negative-charge density allows electrostatic attraction with polycations. Polycationic iridium(III)-containing conjugated metallopolymers such as **MP43** have been designed to detect heparin [113,114]. These polymers exhibited intense blue emission from the backbones and weak red emission from the iridium(III) complexes due to inefficient energy transfer in an aqueous solution. Electrostatic attraction with heparin stabilized a compact conformation of the metallopolymers, which significantly enhanced the energy transfer efficiency, resulting in emission quenching of the blue emission and enhancement of the red emission. The sensitivity of heparin detection was considerably increased via time-resolved photoluminescence technique. **MP43** has also been used for specific labeling of cell membrane via confocal luminescence microscopy and PLIM [114]. Another

iridium(III)-containing conjugated polyelectrolyte (**MP44**) has been designed as a ratiometric protein sensor [115]. It displayed backbone-based fluorescence at 430 nm and iridium-based phosphorescence at 605 nm. The phosphorescence became more intense with increasing polymer concentration, because of the aggregation-induced FRET from polymer backbone to the iridium(III) complex. Interestingly, **MP44** showed fluorescence enhancement but the phosphorescence quenching in the presence of histone, because the strong interaction with histone broke the self-aggregation of **MP44**, and thus minimized the FRET process. Importantly, the luminescence response is in preference to other proteins including a-fetoprotein, bovine serum albumin, thrombin, glucose oxidase, lysozyme, cytochrome c, hemoglobin, and myoglobin, rendering **MP44** a selective ratiometric sensor for histone.

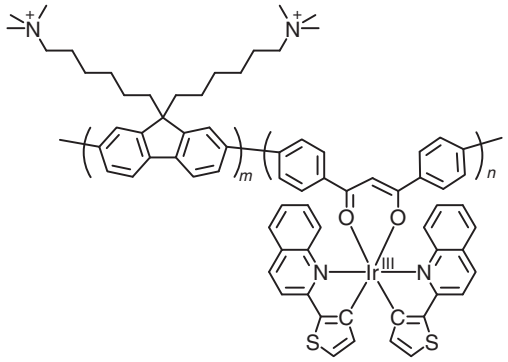

MP43

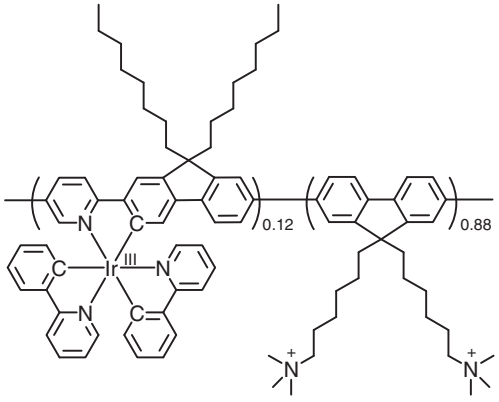

MP44

Cobaltocenium-containing polymers have been reported to show drastic diffrence in hydrophobicity with different anionic counterions [116–118]. With hexafluorophosphate and tetraphenylborate, these metallopolymers are relatively hydrophobic. In contrast, polymers with counterions such as chloride, bromide and nitrate are very hydrophilic. The cobaltocenium-containing polymer **MP45** with the hexafluorophosphate counterion underwent conversion from an organogel to a hydrogel upon ion exchange with tetrabutylammonium chloride [118]. Field-emission scanning electron microscopy indicated that the chloride gel was porous, while the hexafluorophosphate gel appeared much more compact. Since the cationic cobaltocenium can strongly bind to β-lactam antibiotics via ion pairing with carboxylates, **MP45**-Cl was used to recycle antibiotics from water. Additionally, **MP45**-Cl showed inhibition of the growth for Gram-negative *E. coli*, Gram-positive *S. aureus*, and hospital-acquired methicillin-resistant *S. aureus*, probably due to disruption of negative charged cell walls of these bacteria. These results indicated that **MP45**-Cl can not only absorb antibiotics in contaminated water, but also inhibit the growth of drug-resistant bacteria in their environment.

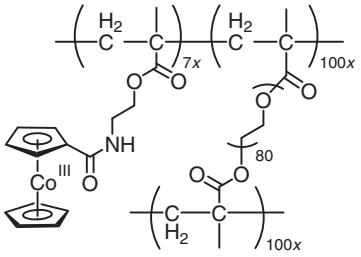

MP45

5. Conclusion

In this Review article, we have summarized recent studies of metallopolymers that are responsive to physical stimuli including temperature, electricity, light, and chemical analytes including pH values, gas molecules, and ions. Their applications in biological sensing and bioimaging have also been discussed. The combination of advantageous features of coordination metal complexes and polymers opens up new directions in the design of novel advanced materials with great application potentials. For example, (1) in the design of thermal responsive materials, polymers respond to temperature change giving conformational conversion, and coordination metal complexes convert the information into visual signals such as absorbance change; (2) in the information storage devices, polymers provide electric conductance, and the various redox states of coordination metal complexes are responsible for recording data; (3) in the chemosensing applications, the analyte-dependent energy and/or electron transfer between polymers and coordination metal complexes results in excellent sensitivity; (4) in the intracellular and *in vivo* applications, polymers increase the water solubility and biocompatibility and long-lived luminescence from metal complexes is distinguishable from short-lived autofluorescence interference. In the future development of stimuli–responsive metallopolymers, polymerization-based signal amplification will provide an efficient strategy to improve sensitivity. Design of charged metallopolymers that allows electronic attraction with analytes with the opposite charge will improve the specific interaction. For luminescent metallopolymers for bioimaging, tuning the excitation and emission wavelength to lower energy is of particular importance with regard to reducing autofluorescence and photodamage. In conclusion, we anticipate that the interesting properties of metallopolymers will continue to contribute to the development of stimuli–responsive materials.

Acknowledgements

The authors acknowledge the financial support from the National Program for Support of Top-Notch Young Professionals, National Natural Science Foundation of China (61274018, 61136003, and 21501098), Scientific and Technological Innovation Teams of Colleges and Universities in Jiangsu Province (TJ215006), Priority Academic Program Development of Jiangsu Higher Education Institutions, Synergetic Innovation Center for Organic Electronics and Information Displays, Natural Science Foundation of Jiangsu Province of China (BK20130038, BK20150833 and

BM2012010) and Nanjing University of Posts and Telecommunications (NY213097 and NY214083).

References

[1] L. Dong, A.K. Agarwal, D.J. Beebe, H.R. Jiang, Nature 442 (2006) 551.
[2] M.A.C. Stuart, W.T.S. Huck, J. Genzer, M. Muller, C. Ober, M. Stamm, G.B. Sukhorukov, I. Szleifer, V.V. Tsukruk, M. Urban, Nat. Mater. 9 (2010) 101.
[3] S. Mura, J. Nicolas, P. Couvreur, Nat. Mater. 12 (2013) 991.
[4] L. Besnard, F. Marchal, J.F. Paredes, J. Daillant, N. Pantoustier, P. Perrin, P. Guenoun, Adv. Mater. 25 (2013) 2844.
[5] Y. Hoshino, R.C. Ohashi, Y. Miura, Adv. Mater. 26 (2014) 3718.
[6] L. Qiu, D. Liu, Y. Wang, C. Cheng, K. Zhou, J. Ding, V.-T. Truong, D. Li, Adv. Mater. 26 (2014) 3333.
[7] X. Ma, H. Tian, Acc. Chem. Res. 47 (2014) 1971.
[8] L. Isaacs, Acc. Chem. Res. 47 (2014) 2052.
[9] A. Higuchi, Q.-D. Ling, S.S. Kumar, Y. Chang, T.-C. Kao, M.A. Munusamy, A.A. Alarfaj, S.T. Hsu, A. Umezawa, Prog. Polym. Sci. 39 (2014) 1585.
[10] D.S. Kim, J.L. Sessler, Chem. Soc. Rev. 44 (2015) 532.
[11] I. Manners, Science 294 (2001) 1664.
[12] G.R. Whittell, I. Manners, Adv. Mater. 19 (2007) 3439.
[13] Q. Zhao, S.-J. Liu, W. Huang, Macromol. Rapid Commun. 31 (2010) 794.
[14] G.R. Whittell, M.D. Hager, U.S. Schubert, I. Manners, Nat. Mater. 10 (2011) 176.
[15] S.-J. Liu, Y. Chen, W.-J. Xu, Q. Zhao, W. Huang, Macromol. Rapid Commun. 33 (2012) 461.
[16] R. Schroot, C. Friebe, E. Altuntas, S. Crotty, M. Jäger, U.S. Schubert, Macromolecules 46 (2013) 2039.
[17] S. Bode, L. Zedler, F.H. Schacher, B. Dietzek, M. Schmitt, J. Popp, M.D. Hager, U.S. Schubert, Adv. Mater. 25 (2013) 1634.
[18] S.P.-Y. Li, C.T.-S. Lau, M.-W. Louie, Y.-W. Lam, S.H. Cheng, K.K.-W. Lo, Biomaterials 34 (2013) 7519.
[19] D.W.R. Balkenende, S. Coulibaly, S. Balog, Y.C. Simon, G.L.C. Weder, J. Am. Chem. Soc. 136 (2014) 10493.
[20] I. Cobo, M. Li, B.S. Sumerlin, S. Perrier, Nat. Mater. 14 (2015) 143.
[21] W.-Y. Wong, Dalton Trans (2007) 4495.
[22] W.-Y. Wong, C.-L. Ho, Coord. Chem. Rev. 250 (2006) 2627.
[23] C.-L. Ho, W.-Y. Wong, Coord. Chem. Rev. 255 (2011) 2469.
[24] C.-L. Ho, W.-Y. Wong, Coord. Chem. Rev. 257 (2013) 1614.
[25] W.-Y. Wong, P.D. Harvey, Macromol. Rapid Commun. 31 (2010) 671.
[26] J. Xiang, C.-L. Ho, W.-Y. Wong, Polym. Chem. 6 (2015) 6905.
[27] W.-Y. Wong, C.-L. Ho, Acc. Chem. Res. 43 (2010) 1246.
[28] W.-Y. Wong, Macromol. Chem. Phys. 209 (2008) 14.
[29] G.-J. Zhou, W.-Y. Wong, Chem. Soc. Rev. 40 (2011) 2541.
[30] J. Liu, Y. Liu, Q. Liu, C. Li, L. Sun, F. Li, J. Am. Chem. Soc. 133 (2011) 15276.
[31] D.-L. Ma, D.S.-H. Chan, C.-H. Leung, Acc. Chem. Res. 47 (2014) 3614.
[32] L. Lu, D.S.-H. Chan, D.W.J. Kwong, H.-Z. He, C.-H. Leung, D.-L. Ma, Chem. Sci. 5 (2014) 4561.
[33] K.-H. Leung, H.-Z. He, B. He, H.-J. Zhong, S. Lin, Y.-T. Wang, D.-L. Ma, C.-H. Leung, Chem. Sci. 6 (2015) 2166.
[34] S. Lin, W. Gao, Z. Tian, C. Yang, L. Lu, J.-L. Mergny, C.-H. Leung, D.-L. Ma, Chem. Sci. 6 (2015) 4284.
[35] S.W. Botchway, M. Charnley, J.W. Haycock, A.W. Parker, D.L. Rochester, J.A. Weinstein, J.A.G. Williams, Proc. Natl. Acad. Sci. U.S.A. 105 (2008) 16071.
[36] Y. You, S.Y. Park, Adv. Mater. 20 (2008) 3820.
[37] Q. Zhao, F.Y. Li, C.H. Huang, Chem. Soc. Rev. 39 (2010) 3007.
[38] Q. Zhao, C. Huang, F. Li, Chem. Soc. Rev. 40 (2011) 2508.
[39] C.P. Montgomery, B.S. Murray, E.J. New, R. Pal, D. Parker, Acc. Chem. Res. 42 (2009) 925.
[40] J.-C.G. Bünzli, Chem. Rev. 110 (2010) 2729.
[41] X. de Hatten, N. Bell, N. Yufa, G. Christmann, J.R. Nitschke, J. Am. Chem. Soc. 133 (2011) 3158.
[42] D. Asil, J.A. Foster, A. Patra, X. de Hatten, J. del Barrio, O.A. Scherman, J.R. Nitschke, R.H. Friend, Angew. Chem. Int. Ed. 53 (2014) 8388.
[43] K. Miyata, Y. Konno, T. Nakanishi, A. Kobayashi, M. Kato, K. Fushimi, Y. Hasegawa, Angew. Chem. Int. Ed. 52 (2013) 6413.
[44] F. Pinaud, L. Russo, S. Pinet, I. Gosse, V. Ravaine, N. Sojic, J. Am. Chem. Soc. 135 (2013) 5517.
[45] H. Sun, S. Liu, W. Lin, K.Y. Zhang, W. Lv, X. Huang, F. Huo, H. Yang, G. Jenkins, Q. Zhao, W. Huang, Nat. Commun. 5 (2014) 3601.
[46] P.M. Beauiuge, J.R. Reynolds, Chem. Rev. 110 (2010) 268.
[47] C. He, J. Li, X. Wu, P. Chen, J. Zhao, K. Yin, M. Cheng, W. Yang, G. Xie, D. Wang, D. Liu, R. Yang, D. Shi, Z. Li, L. Sun, G. Zhang, Adv. Mater. 25 (2013) 5593.
[48] A.B. Powell, C.W. Bielawski, A.H. Cowley, J. Am. Chem. Soc. 132 (2010) 10184.
[49] C.M. Amb, A.L. Dyer, J.R. Reynolds, Chem. Mater. 23 (2011) 397.
[50] S. Inagi, H. Nagai, I. Tomita, T. Fuchigami, Angew. Chem. Int. Ed. 52 (2013) 6616.
[51] Q. Zeng, A. McNally, T.E. Keyes, R.J. Forster, Electrochem. Commun. 10 (2008) 466.
[52] B.-B. Cui, C.-J. Yao, J. Yao, Y.-W. Zhong, Chem. Sci. 5 (2014) 932.
[53] C.-W. Hu, T. Sato, J. Zhang, S. Moriyama, M. Higuchi, J. Mater. Chem. C 1 (2013) 3408.
[54] J. Matsui, R. Kikuchi, T. Miyashita, J. Am. Chem. Soc. 136 (2014) 842.
[55] T.-L. Choi, K.-H. Lee, W.-J. Joo, S. Lee, T.-W. Lee, M.Y. Chae, J. Am. Chem. Soc. 129 (2007) 9842.
[56] J. Xiang, T.-K. Wang, Q. Zhao, W. Huang, C.-L. Ho, W.-Y. Wong, J. Mater. Chem. C 4 (2016) 921.
[57] M.A. Hempenius, C. Cirmi, F. Lo Savio, J. Song, G.J. Vancso, Macromol. Rapid Commun. 31 (2010) 772.
[58] J.-C. Eloi, D.A. Rider, G. Cambridge, G.R. Whittell, M.A. Winnik, I. Manners, J. Am. Chem. Soc. 133 (2011) 8903.
[59] K. Zhang, X. Feng, X. Sui, M.A. Hempenius, G.J. Vancso, Angew. Chem. Int. Ed. 53 (2014) 13789.
[60] S.-J. Liu, W.-P. Lin, M.-D. Yi, W.-J. Xu, C. Tang, Q. Zhao, S.-H. Ye, X.-M. Liu, W. Huang, J. Mater. Chem. 22 (2012) 22964.
[61] S.-J. Liu, Z.-H. Lin, Q. Zhao, Y. Ma, H.-F. Shi, M.-D. Yi, Q.-D. Ling, Q.-L. Fan, C.-X. Zhu, E.-T. Kang, W. Huang, Adv. Funct. Mater. 21 (2011) 979.
[62] P. Wang, S.-J. Liu, Z.-H. Lin, X.-C. Dong, Q. Zhao, W.-P. Lin, M.-D. Yi, S.-H. Ye, C.-X. Zhu, W. Huang, J. Mater. Chem. 22 (2012) 9576.
[63] W. Lin, H. Sun, S. Liu, H. Yang, S. Ye, W. Xu, Q. Zhao, X. Liu, W. Huang, Macromol. Chem. Phys. 213 (2012) 2472.
[64] S.L. Lim, Q. Ling, E.Y.H. Teo, C.X. Zhu, D.S.H. Chan, E.-T. Kang, K.G. Neoh, Chem. Mater. 19 (2007) 5148.
[65] S.-J. Liu, P. Wang, Q. Zhao, H.-Y. Yang, J. Wong, H.-B. Sun, X.-C. Dong, W.-P. Lin, W. Huang, Adv. Mater 24 (2012) 2901.
[66] F.D. Jochum, P. Theato, Polymer 50 (2009) 3079.
[67] F.D. Jochum, F.R. Forst, P. Theato, Macromol. Rapid Commun. 31 (2010) 1456.
[68] Z. Mahimwalla, K.G. Yager, J.-I. Mamiya, A. Shishido, A. Priimagi, C.J. Barrett, Polym. Bull. 69 (2012) 967.
[69] M. Dong, A. Babalhavaeji, S. Samanta, A.A. Beharry, G.A. Woolley, Acc. Chem. Res. 48 (2015) 2662.
[70] D. Bleger, S. Hecht, Angew. Chem. Int. Ed. 54 (2015) 11338.
[71] E.C. Harvey, B.L. Feringa, J.G. Vos, W.R. Browne, M.T. Pryce, Coord. Chem. Rev. 282 (2015) 77.
[72] M. Irie, T. Fulcaminato, K. Matsuda, S. Kobatake, Chem. Res. 114 (2014) 12174.
[73] E. Borré, J.-F. Stumbé, S. Bellemin-Laponnaz, M. Mauro, Angew. Chem. Int. Ed. 55 (2016) 1313.
[74] G. Cosquer, M. Morimoto, M. Irie, A. Fetoh, B.K. Breedlove, M. Yamashita, Dalton Trans. 44 (2015) 5996.
[75] J. Li, F. Song, L. Wang, J. Jiao, Y. Cheng, C. Zhu, Macromol. Rapid Commun. 33 (2012) 1268.
[76] E.S. Gil, S.M. Hudson, Prog. Polym. Sci. 29 (2004) 1173.
[77] K.L. Robinson, N.S. Lawrence, Anal. Chem. 78 (2006) 2450.
[78] F. Wilkinson, A.A. Abdel-Shafi, J. Phys. Chem. A 103 (1999) 5425.
[79] C.S.K. Mak, D. Pentlehner, M. Stich, O.S. Wolfbeis, W.K. Chan, H. Yersin, Chem. Mater. 21 (2009) 2173.
[80] A. Habibagahi, Y. Mébarki, Y. Sultan, G.P.A. Yap, R.J. Crutchley, ACS Appl. Mater. Interfaces 1 (2009) 1785.
[81] S.W. Thomas III, S. Yagi, T.M. Swager, J. Mater. Chem. 15 (2005) 2829.
[82] H. Xiang, L. Zhou, Y. Feng, J. Cheng, D. Wu, X. Zhou, Inorg. Chem. 51 (2012) 5208.
[83] F. Murad, Angew. Chem. Int. Ed. 38 (1999) 1856.
[84] R.F. Furchgott, Angew. Chem. Int. Ed. 38 (1999) 1870.
[85] L.J. Ignarro, Angew. Chem. Int. Ed. 38 (1999) 1882.
[86] G. Clermont, S. Lecour, C. Vergely, M. Zeller, C. Perrin, V. Maupoil, O. Bouchot, L. Rochette, Fundam. Clin. Pharmacol. 17 (2003) 709.
[87] R.C. Smith, A.G. Tennyson, A.C. Won, S.J. Lippard, Inorg. Chem. 45 (2006) 9367.
[88] L. Do, R.C. Smith, A.G. Tennyson, S.J. Lippard, Inorg. Chem. 45 (2006) 8998.
[89] B.J. Holliday, T.B. Stanford, T.M. Swager, Chem. Mater. 18 (2006) 5649.
[90] H. Masai, J. Terao, S. Seki, S. Nakashima, M. Kiguchi, K. Okoshi, T. Fujihara, Y. Tsuji, J. Am. Chem. Soc. 136 (2014) 1742.
[91] X. Feng, X. Sui, M.A. Hempenius, G.J. Vancso, J. Am. Chem. Soc. 136 (2014) 7865.
[92] K.Y. Zhang, J. Zhang, Y. Liu, S. Liu, P. Zhang, Q. Zhao, Y. Tang, W. Huang, Chem. Sci. 6 (2015) 301.
[93] K.Y. Zhang, H.-W. Liu, M.-C. Tang, A.W.-T. Choi, N. Zhu, X.-G. Wei, K.-C. Lau, K.K.-W. Lo, Inorg. Chem. 54 (2015) 6582.
[94] H.-F. Shi, S.-J. Liu, H.-B. Sun, W.-J. Xu, Z.-F. An, J. Chen, S. Sun, X.-M. Lu, Q. Zhao, W. Huang, Chem. Eur. J. 16 (2010) 12158.
[95] H. Shi, S. Liu, Z. An, H. Yang, J. Geng, Q. Zhao, B. Liu, W. Huang, Macromol. Biosci. 13 (2013) 1339.
[96] H. Tan, B. Liu, Y. Chen, ACS Nano 6 (2012) 11505.
[97] C. Deraedt, A. Rapakousiou, Y. Wang, L. Salmon, M. Bousquet, D. Astruc, Angew. Chem. Int. Ed. 53 (2014) 8445.
[98] C. Qin, W.-Y. Wong, L. Wang, Macromolecules 44 (2011) 483.
[99] L.-J. Fan, Y. Zhang, W.E. Jones Jr., Macromolecules 38 (2005) 2844.
[100] M.E.A. Fegley, T. Sandgren, J.L. Duffy-Matzner, A. Chen, W.E. Jones Jr., J. Polym. Sci. Pol. Chem. 53 (2015) 951.
[101] H. Liu, H. Yang, X. Hao, H. Xu, Y. Lv, D. Xiao, H. Wang, Z. Tian, Small 9 (2013) 2639.
[102] H. Shi, X. Ma, Q. Zhao, B. Liu, Q. Qu, Z. An, Y. Zhao, W. Huang, Adv. Funct. Mater. 24 (2014) 4823.
[103] Q. Zhao, X. Zhou, T. Cao, K.Y. Zhang, L. Yang, S. Liu, H. Liang, H. Yang, F. Li, W. Huang, Chem. Sci. 6 (2015) 1825.
[104] X. Zheng, X. Wang, H. Mao, W. Wu, B. Liu, X. Jiang, Nat. Commun. 6 (2015) 5834.
[105] S. Kubik, Chem. Soc. Rev. 39 (2010) 3648.
[106] Q. Zhao, C. Zhang, S. Liu, Y. Liu, K.Y. Zhang, X. Zhou, J. Jiang, W. Xu, T. Yang, W. Huang, Sci. Rep. 5 (2015) 16420.
[107] D.E. Fomenko, W. Xing, B.M. Adair, D.J. Thomas, V.N. Gladyshev, Science 315 (2007) 387.

[108] E. Weerapana, C. Wang, G.M. Simon, F. Richter, S. Khare, M.B.D. Dillon, D.A. Bachovchin, K. Mowen, D. Baker, B.F. Cravatt, Nature 468 (2010) 790.
[109] Y. Zhou, J. Yoon, Chem. Soc. Rev. 41 (2012) 52.
[110] Z.Q. Guo, S.W. Nam, S. Park, J. Yoon, Chem. Sci. 3 (2012) 2760.
[111] S. Liu, W. Qiao, G. Cao, Y. Chen, Y. Ma, Y. Huang, X. Liu, W. Xu, Q. Zhao, W. Huang, Macromol. Rapid Commun. 34 (2013) 81.
[112] Y. Ma, S. Liu, H. Yang, Y. Wu, H. Sun, J. Wang, Q. Zhao, F. Li, W. Huang, J. Mater. Chem. B 1 (2013) 319.
[113] H. Shi, X. Chen, S. Liu, H. Xu, Z. An, L. Ouyang, Z. Tu, Q. Zhao, Q. Fan, L. Wang, W. Huang, ACS Appl. Mater. Interfaces 5 (2013) 4562.
[114] H. Shi, H. Sun, H. Yang, S. Liu, G. Jenkins, W. Feng, F. Li, Q. Zhao, B. Liu, W. Huang, Adv. Funct. Mater. 23 (2013) 3268.
[115] P. Sun, X. Lu, Q. Fan, Z. Zhang, W. Song, B. Li, L. Huang, J. Peng, W. Huang, Macromolecules 44 (2011) 8763.
[116] J. Zhang, Y. Yan, M.W. Chance, J. Chen, J. Hayat, S. Ma, C. Tang, Angew. Chem. Int. Ed. 52 (2013) 13387.
[117] J. Zhang, P.J. Pellechia, J. Hayat, C.G. Hardy, C. Tang, Macromolecules 46 (2013) 1618.
[118] J. Zhang, J. Yan, P. Pageni, Y. Yan, A. Wirth, Y.-P. Chen, Y. Qiao, Q. Wang, A.W. Decho, C. Tang, Sci. Rep. 5 (2015) 11914.